Electronic Supplementary Material (ESI) for Chemical Communications.

Supplementary Information for

Local Density Changes and Carbonate Rotation Enable Ba Incorporation in Amorphous Calcium Carbonate

Sebastien N. Kerisit, Micah P. Prange, and Sebastian T. Mergelsberg*

Physical and Computational Sciences Directorate, Pacific Northwest National Laboratory, Richland, Washington 99352, United States.

*Email: sebastien.kerisit@pnnl.gov

Computational Methods

Ab initio molecular dynamics (AIMD) simulations based on density functional theory (DFT) were performed with VASP (Vienna ab initio Simulation Package)[1-4] using the projector augmented-wave (PAW) approach[5, 6] and the Perdew, Burke, Ernzerhof[7, 8] (PBE) approximate exchange-correlation functional augmented by the Grimme dispersion corrections (D3).[9, 10] The PBE PAW potentials from the VASP database for H, C, O, Ca, and Ba were used. These remove 0, 2, 2, 12, and 46 electrons from the DFT calculation for each element, respectively. AIMD simulations were performed in the *NVT* (constant number of particles, constant volume, and constant temperature) and *NPT* (constant pressure) ensembles with an integration time step of 0.5 fs and at the Γ point (1 × 1 × 1 *k*-point mesh). The temperature was fixed by a Nosé–Hoover thermostat[11, 12] with the fictitious mass set to 3.0 for *NVT* runs. In *NPT* calculations, a Langevin thermostat[13] with damping coefficient of 10 ps^{-1} was used for the atomic degrees of freedom and a Langevin barostat with damping coefficient of also 10 ps^{-1} was used for the lattice degrees of freedom (Parrinello-Rahman dynamics[14, 15]). The convergence criterion for the electronic self-consistent calculation was 10^{-5} eV throughout.

The calculations were performed in (initially) cubic boxes with 24 each of CO_3^{2-} groups, M^{2+} cations (M = Ca, Ba), and H_2O molecules. Initial amorphous configurations were generated by randomly placing the molecular groups on a cubic grid followed by relaxation and equilibration for 1 ns at room temperature with classical molecular dynamics (CMD) using DL_POLY Classic.[16] Simulation parameters for these calculations were the same as in our previous work.[17] The potential parameters for water were those of the flexible SPC model.[18] The parameters that described the intra-carbonate, inter-carbonate, carbonate–water, calcium–carbonate and calcium–water interactions were those in Kerisit and Parker[19] and references therein. The parameters for

the barium–carbonate oxygen and barium–water oxygen interactions were from Raiteri et al.[20] With the volume held constant, these initial CMD structures were melted in AIMD at T = 1500 K and configuration were drawn for the quench stage at regular intervals. The molten configurations, which were prepared using a lower 300 eV energy cutoff, were quenched to room temperature (300 K) at a rate of 300 K ps^{-1} to generate models of the hydrated, amorphous solids. These quenched configurations were then run in the *NVT* ensemble for 12 ps using a 600-eV energy cutoff to accumulate 960 snapshots by sampling the structure every 12.5 fs. Subsequently, the final structures of the *NVT* simulations were used as starting points for 12 ps *NPT* simulations from which another set of 960 snapshots were collected. For ACC(Ba), a molten pure ACC configuration with one Ba atom substituted for one Ca atom was used as the initial configuration instead of following the CMD protocol. For ACC(Ba), the average simulation cell side length was 12.73 Å from the *NPT* simulations.

Definition of orientation order parameter

The distance-dependent orientation order parameter, $S(r)$, is defined as

$$S(r) = \frac{\sum_{i=1}^{N_C} 0.5 \times (3\cos^2\theta_i - 1)}{N_C}$$

where N_C is the number of carbonate ions and θ is the angle between the Ca/Ba–C vector and the normal to the carbonate plane defined by its three O atoms. S equals −0.5, 1, and 0 for edge-on, face-on, and random orientations, respectively.

Radial Distribution Functions (RDFs) of Ca and Ba in ACC(Ba)

Figures S1 through S8 depict RDFs of Ca or Ba with carbonate oxygen (Oc), water oxygen (Ow), carbon (C), or calcium (Ca) atoms obtained from NPT AIMD simulations of Ba incorporated in ACC (ACC(Ba)). In each graph, both the RDFs from individual simulations and the running averages in five-configuration intervals are shown. The running averages help establish convergence of the different RDFs as a function of the number of configurations pulled from the melt.

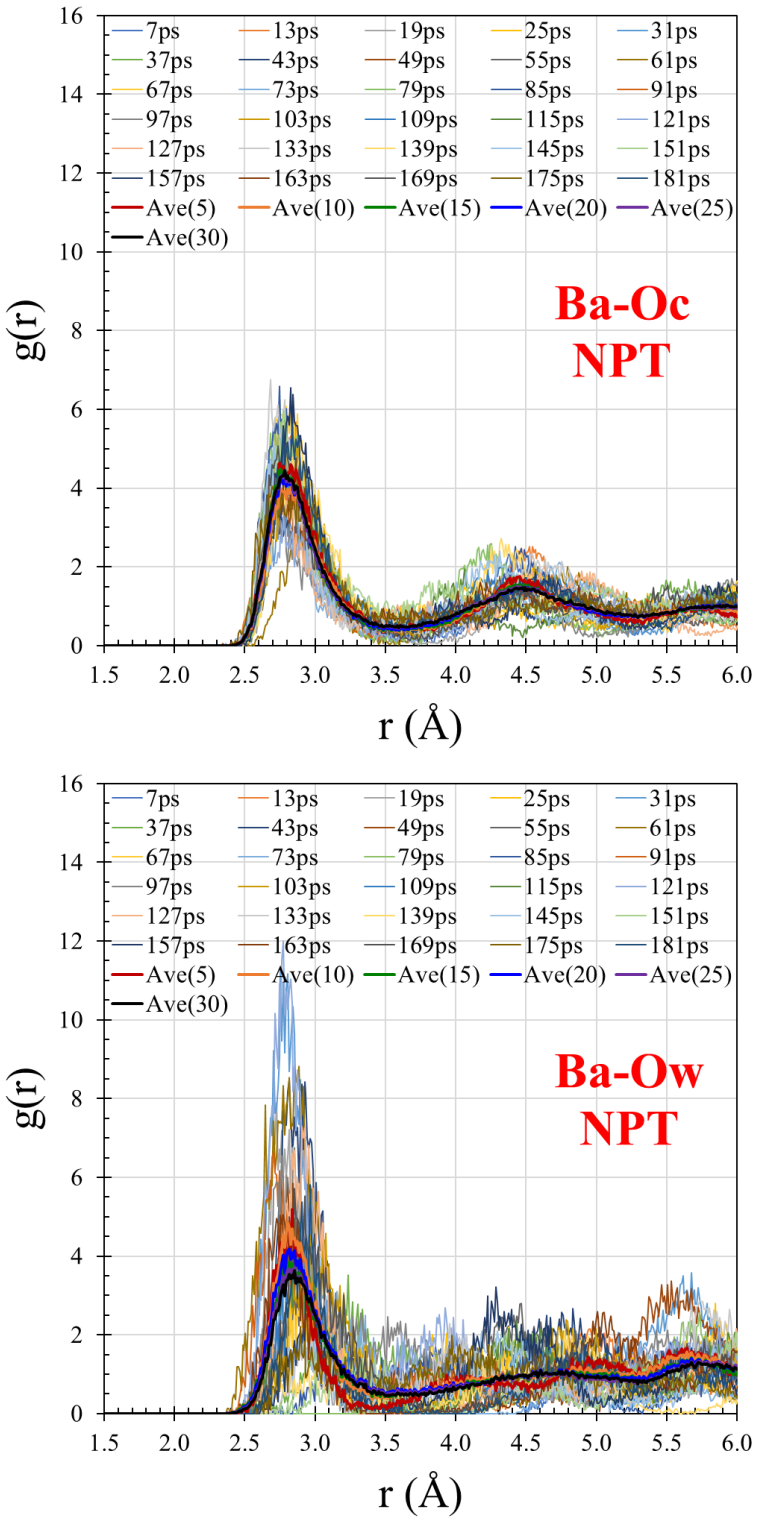

Figure S1. Ba–carbonate O (top) and Ba–water O (bottom) radial distribution functions calculated from the 30 individual NPT simulations (thin lines, denoted by the time at which a configuration was pulled from the melt) and running averages in five-configuration intervals (thick lines, with the number of configurations used in the average shown in parentheses).

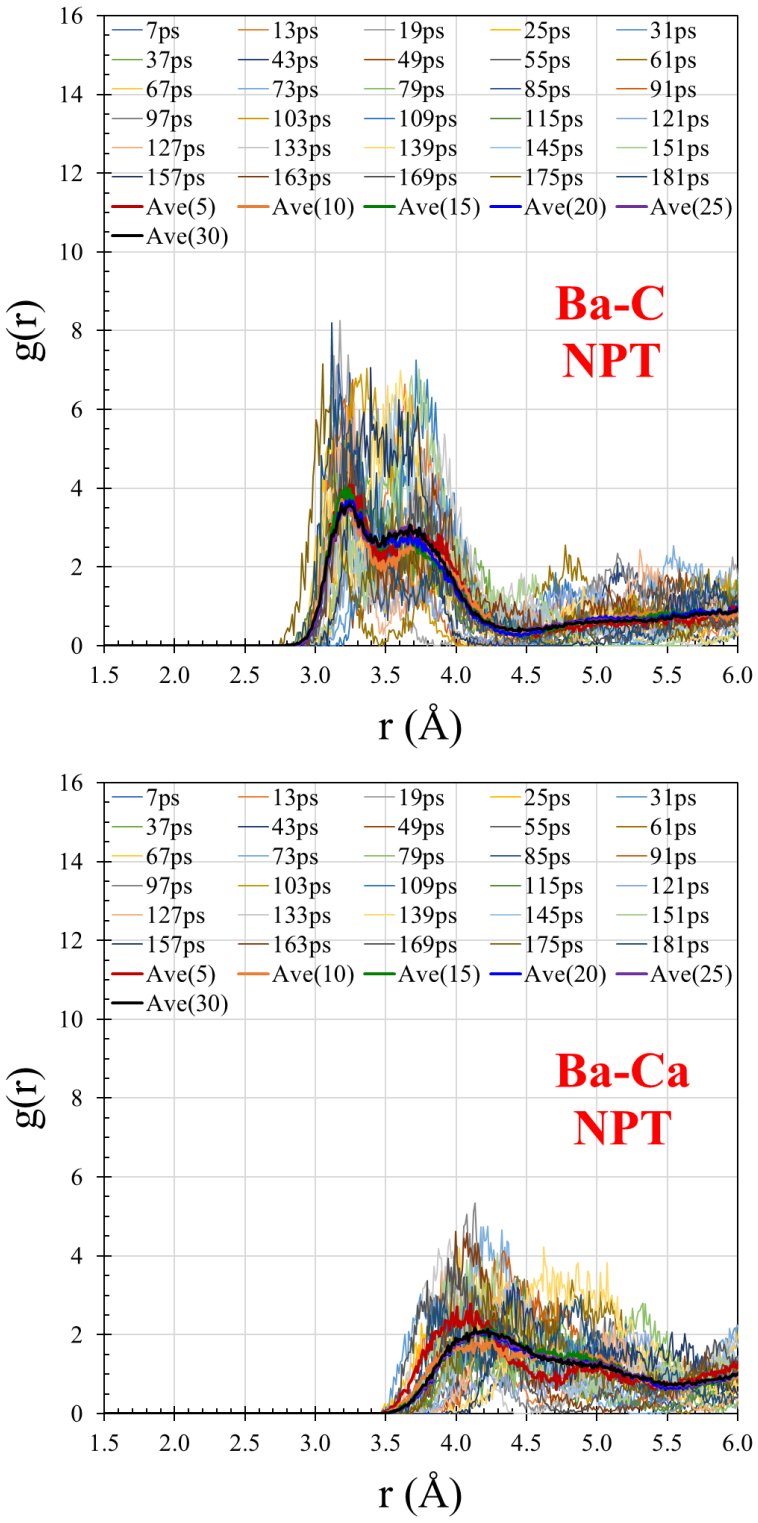

Figure S2. Ba–C (top) and Ba–Ca (bottom) radial distribution functions calculated from the 30 individual NPT simulations (thin lines, denoted by the time at which a configuration was pulled from the melt) and running averages in five-configuration intervals (thick lines, with the number of configurations used in the average shown in parentheses).

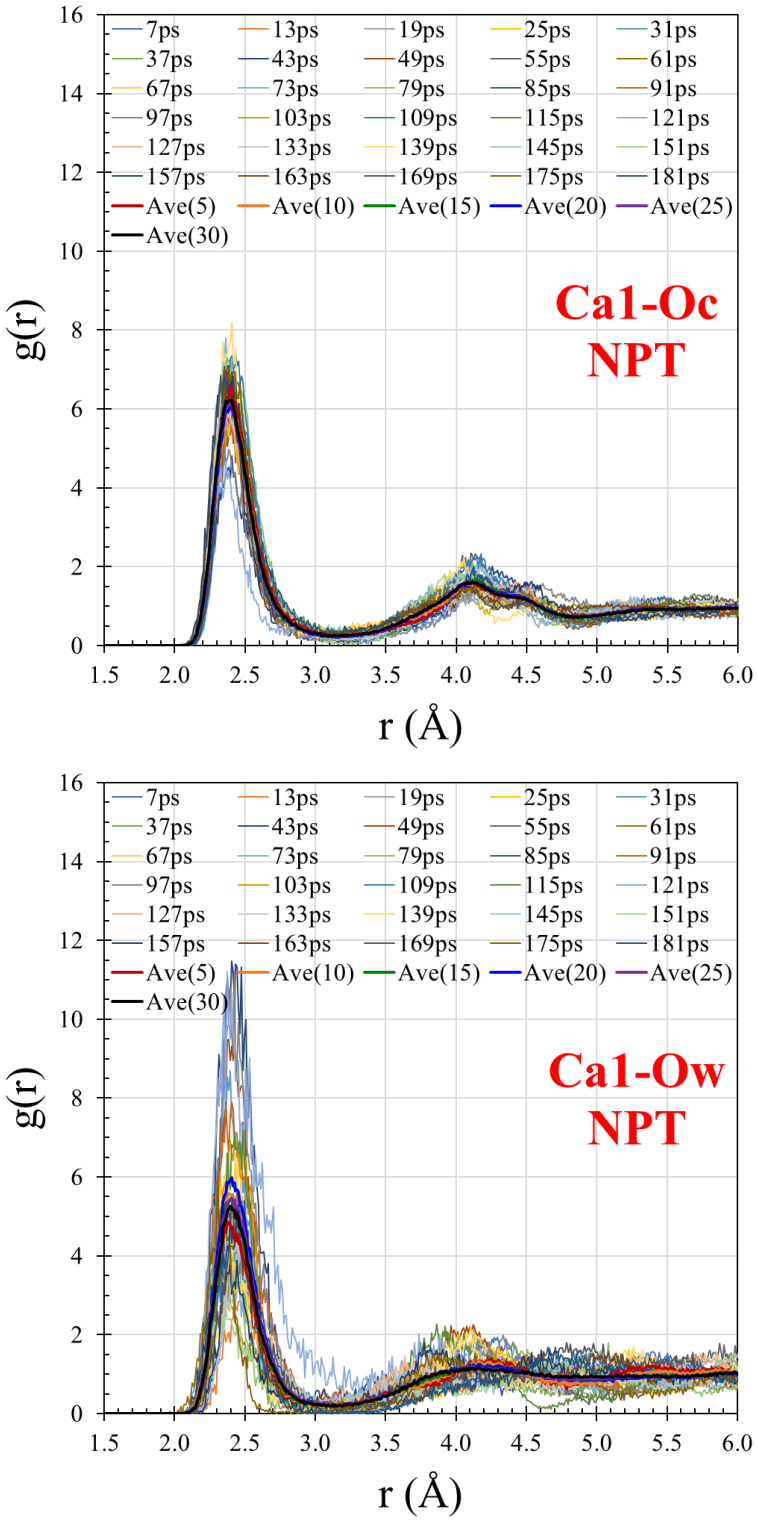

Figure S3. Ca1–carbonate O (top) and Ca1–water O (bottom) radial distribution functions calculated from the 30 individual NPT simulations (thin lines, denoted by the time at which a configuration was pulled from the melt) and running averages in five-configuration intervals (thick lines, with the number of configurations used in the average shown in parentheses).

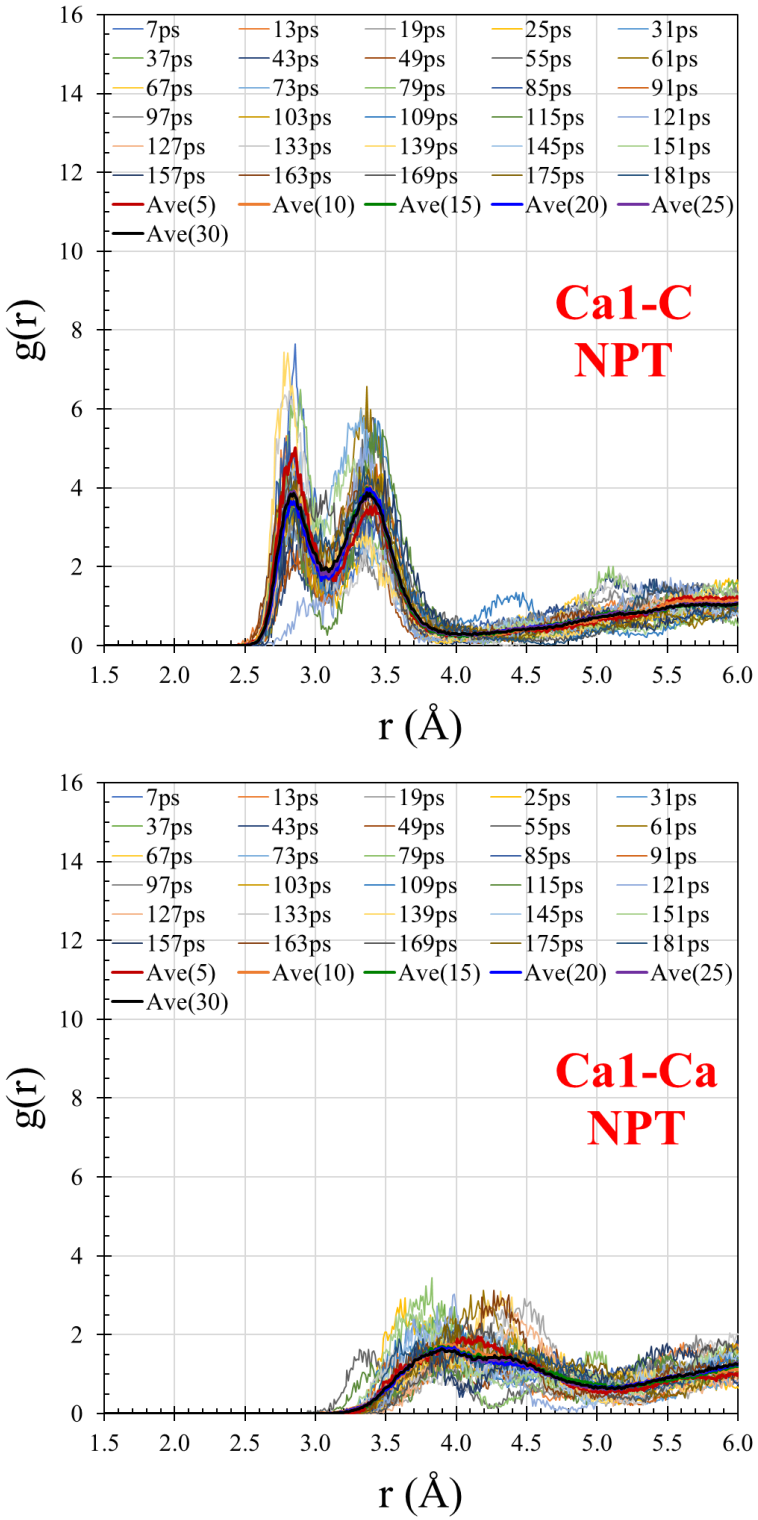

Figure S4. Ca1–C (top) and Ca1–Ca (bottom) radial distribution functions calculated from the 30 individual NPT simulations (thin lines, denoted by the time at which a configuration was pulled from the melt) and running averages in five-configuration intervals (thick lines, with the number of configurations used in the average shown in parentheses).

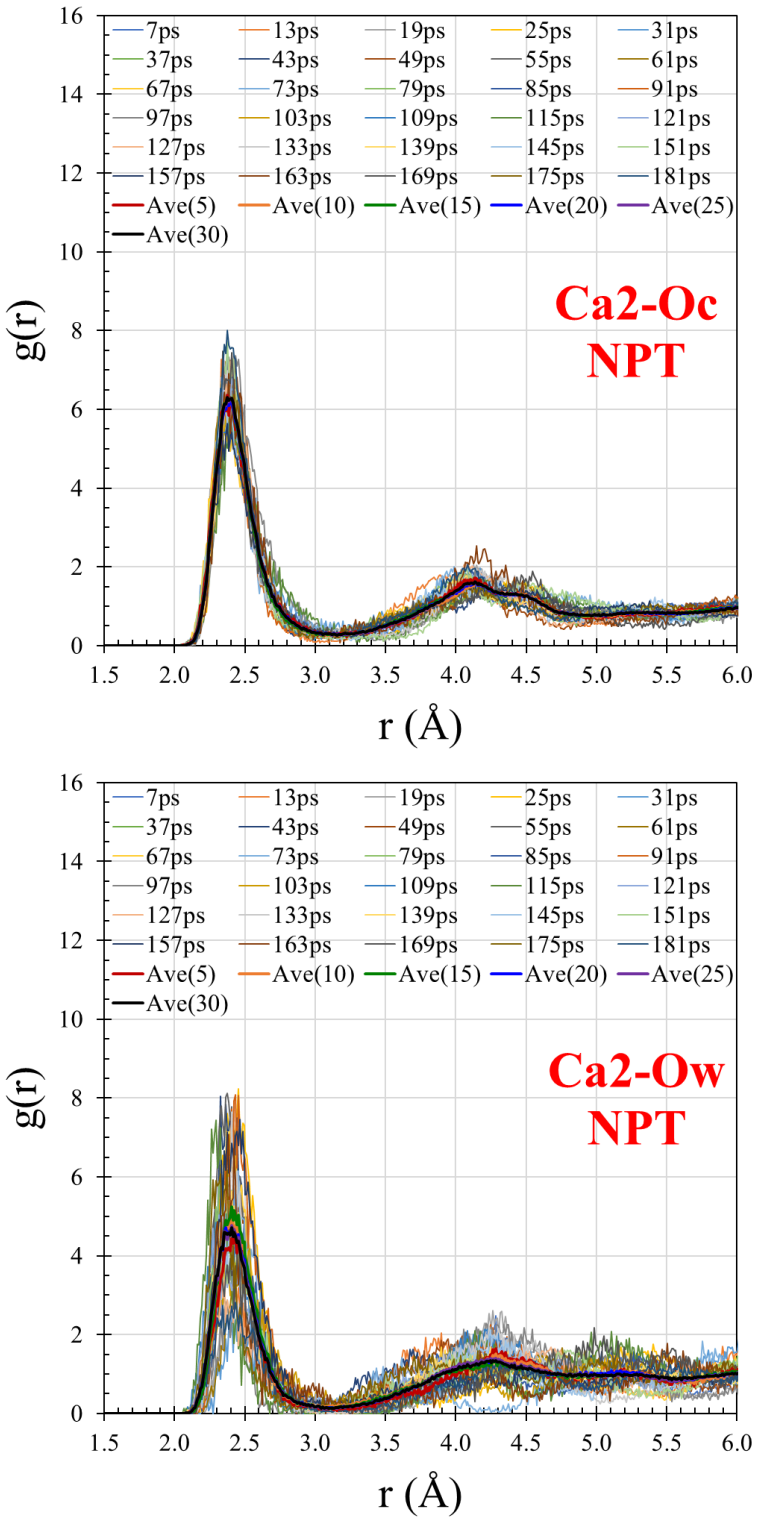

Figure S5. Ca2–carbonate O (top) and Ca2–water O (bottom) radial distribution functions calculated from the 30 individual NPT simulations (thin lines, denoted by the time at which a configuration was pulled from the melt) and running averages in five-configuration intervals (thick lines, with the number of configurations used in the average shown in parentheses).

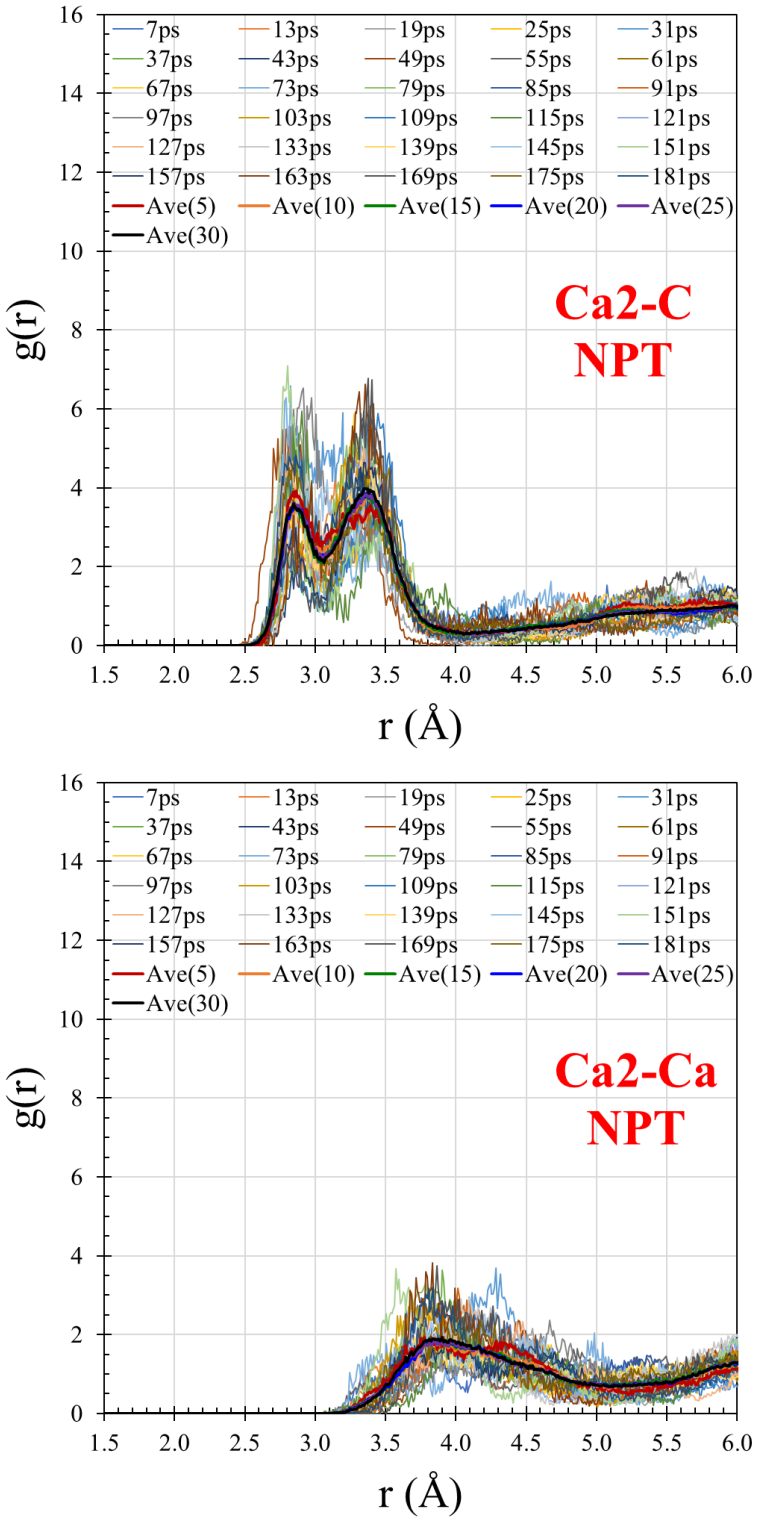

Figure S6. Ca2–C (top) and Ca2–Ca (bottom) radial distribution functions calculated from the 30 individual NPT simulations (thin lines, denoted by the time at which a configuration was pulled from the melt) and running averages in five-configuration intervals (thick lines, with the number of configurations used in the average shown in parentheses).

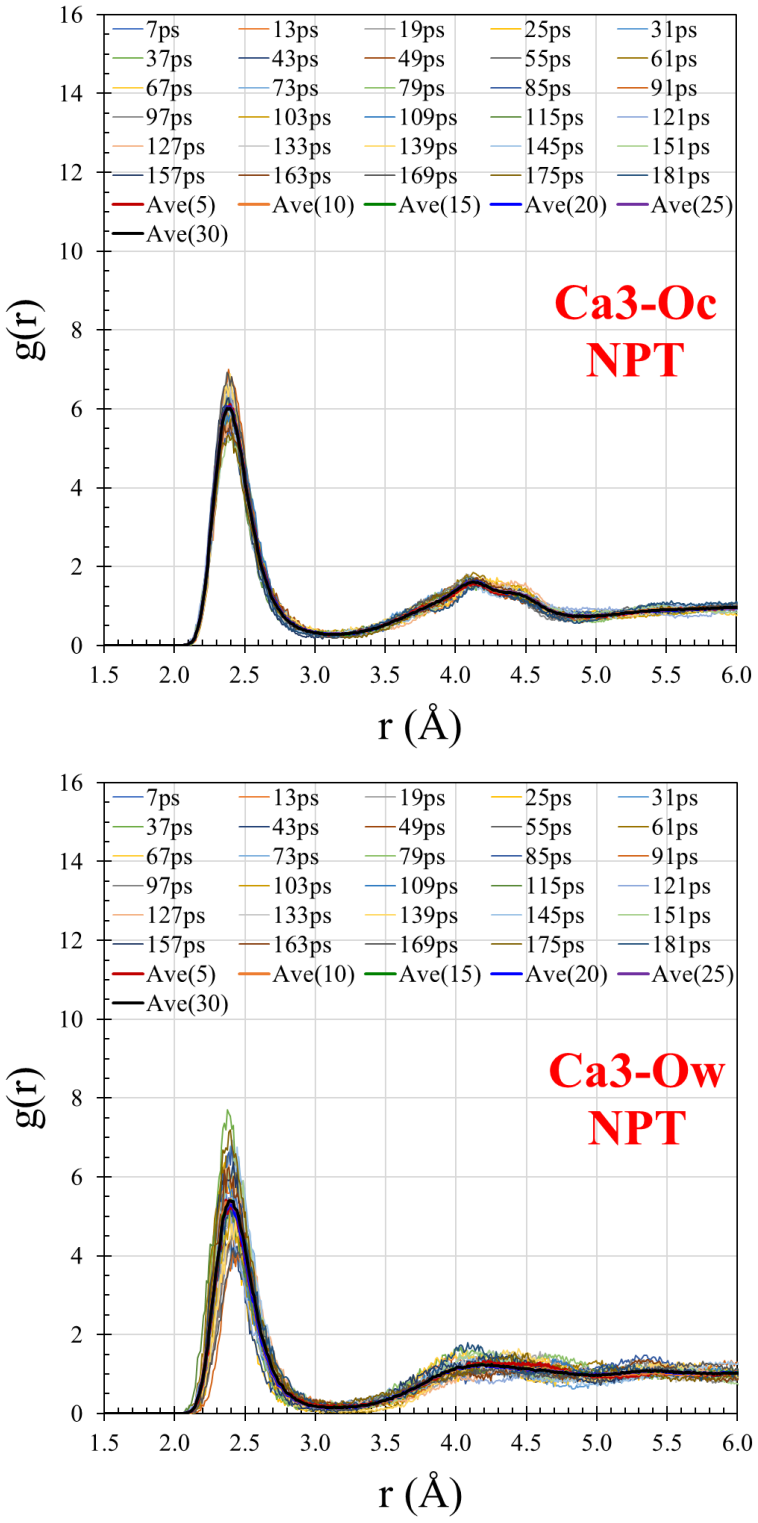

Figure S7. Ca3–carbonate O (top) and Ca3–water O (bottom) radial distribution functions calculated from the 30 individual NPT simulations (thin lines, denoted by the time at which a configuration was pulled from the melt) and running averages in five-configuration intervals (thick lines, with the number of configurations used in the average shown in parentheses).

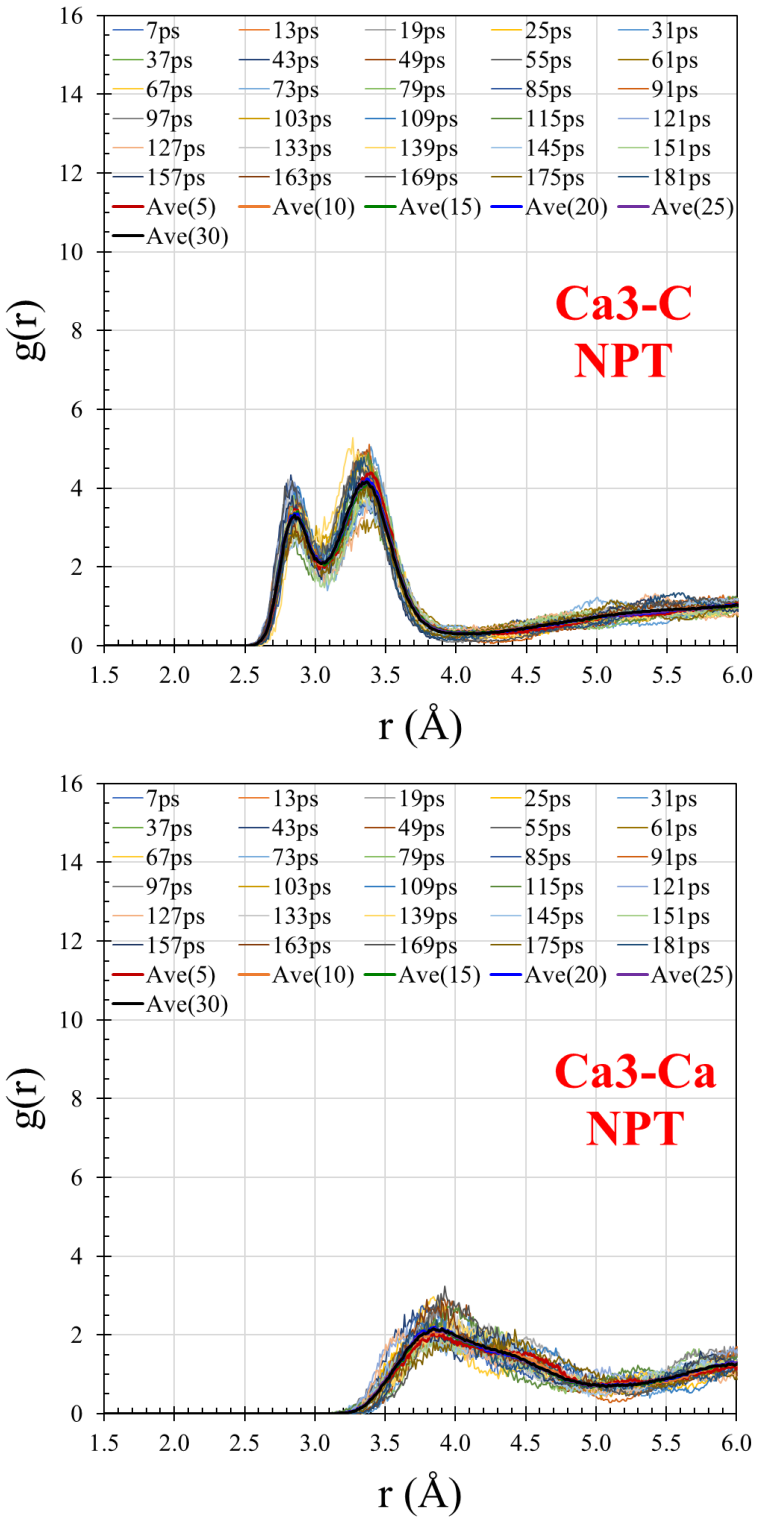

Figure S8. Ca3–C (top) and Ca3–Ca (bottom) radial distribution functions calculated from the 30 individual NPT simulations (thin lines, denoted by the time at which a configuration was pulled from the melt) and running averages in five-configuration intervals (thick lines, with the number of configurations used in the average shown in parentheses).

Incorporation Energetics

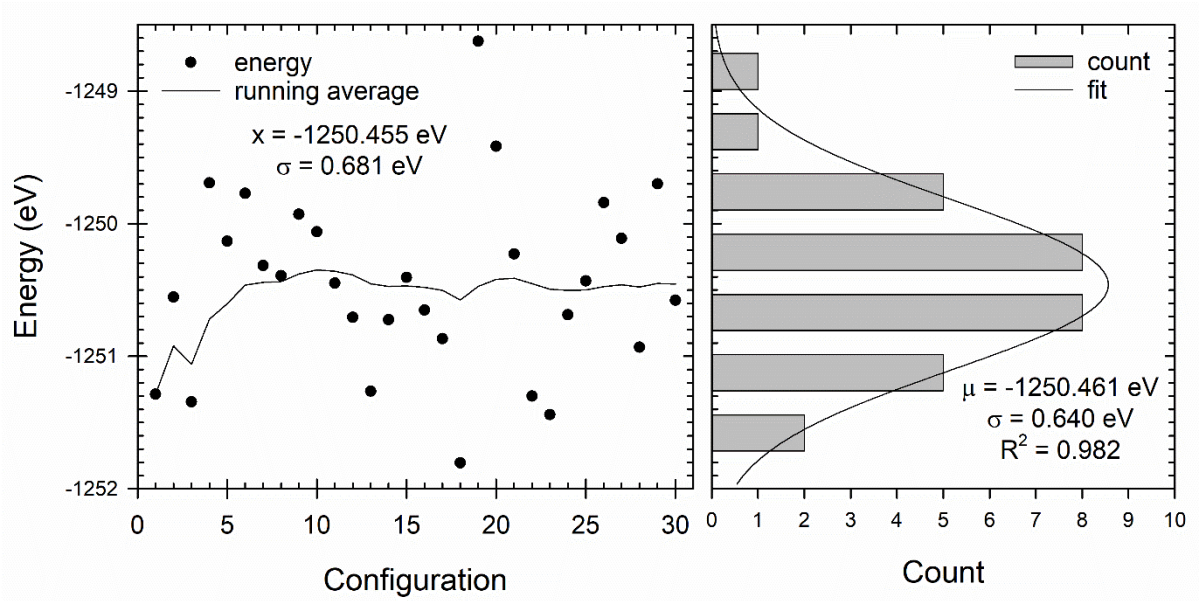

Figure S9. (left) Average internal energy of the ACC(Ba) supercell calculated for the 30 individual NPT simulations. Histogram of the 30 average internal energies together with fit to a normal distribution.

Molar volumes

Table 1. Molar volumes and associated statistics (mean (μ), standard deviation (σ), and standard error of the mean (SEM)) of ACC, ABC, and ACC(Ba).

ACC					
Config. #	**MV (cm^3/mol)**	**Config. #**	**MV (cm^3/mol)**	**Config. #**	**MV (cm^3/mol)**
1	51.98323	3	51.50403	5	51.62787
2	51.35452	4	51.61519	6	50.81179
μ	**51.482**	***σ***	**0.391**	**SEM**	**0.159**
ABC					
Config. #	**MV (cm^3/mol)**	**Config. #**	**MV (cm^3/mol)**	**Config. #**	**MV (cm^3/mol)**
1	63.65344	3	62.67024	5	63.03618
2	63.47994	4	63.03084	6	63.53542
μ	**63.234**	***σ***	**0.381**	**SEM**	**0.156**
ACC(Ba)					
Config. #	**MV (cm^3/mol)**	**Config. #**	**MV (cm^3/mol)**	**Config. #**	**MV (cm^3/mol)**
1	50.89573	11	51.47131	21	51.38604
2	51.05074	12	50.88955	22	51.96763
3	52.51443	13	51.70865	23	51.13519
4	52.28969	14	51.47419	24	51.09412
5	51.05253	15	51.88150	25	51.26768
6	52.32814	16	51.25584	26	52.30160
7	51.31973	17	50.80411	27	51.36907
8	51.02758	18	51.57681	28	52.05321
9	51.85050	19	52.50447	29	51.56917
10	51.75773	20	52.85779	30	51.55700
μ	**51.607**	***σ***	**0.549**	**SEM**	**0.100**

The predicted molar volume of ACC(Ba), assuming an ideal $Ba_xCa_{1-x}CO_3 \cdot H_2O$ solid solution with x=0.04167 (1 out 24 Ca atoms substituted by Ba), is 23/24×51.482+63.234/24=51.972 cm^3/mol with a standard error of $((23/24\times0.159)^2+(0.156/24)^2)^{1/2}$=0.153 cm^3/mol.

References

1. G. Kresse and J. Furthmuller, *Phys. Rev. B*, 1996, **54**, 11169-11186.
2. G. Kresse and J. Furthmuller, *Comp. Mat. Sci.*, 1996, **6**, 15-50.
3. G. Kresse and J. Hafner, *Phys. Rev. B*, 1993, **47**, 558-561.
4. G. Kresse and J. Hafner, *Phys. Rev. B*, 1994, **49**, 14251-14269.
5. P. E. Blöchl, *Phys. Rev. B*, 1994, **50**, 17953-17979.
6. G. Kresse and D. Joubert, *Phys. Rev. B*, 1999, **59**, 1758-1775.
7. J. P. Perdew, K. Burke and M. Ernzerhof, *Phys. Rev. Lett.*, 1996, **77**, 3865-3868.
8. J. P. Perdew, K. Burke and M. Ernzerhof, *Phys. Rev. Lett.*, 1997, **78**, 1396-1396.
9. S. Grimme, *J. Comput. Chem.*, 2006, **27**, 1787-1799.
10. S. Grimme, J. Antony, S. Ehrlich and H. Krieg, *J. Chem. Phys.*, 2010, **132**, 154104.
11. S. Nosé, *J. Chem. Phys.*, 1984, **81**, 511-519.
12. W. G. Hoover, *Phys. Rev. A*, 1985, **31**, 1695-1697.
13. M. P. Allen and D. J. Tildesley, *Computer Simulation of Liquids*, Oxford University Press, Oxford, UK, 1987.
14. M. Parrinello and A. Rahman, *Phys. Rev. Lett.*, 1980, **45**, 1196-1199.
15. M. Parrinello and A. Rahman, *J. Appl. Phys.*, 1981, **52**, 7182-7190.
16. W. Smith and T. R. Forester, *J. Mol. Graphics*, 1996, **14**, 136-141.
17. M. P. Prange, S. T. Mergelsberg and S. N. Kerisit, *Cryst. Growth Des.*, 2021, **21**, 2212-2221.
18. O. Teleman, B. Jönsson and S. Engström, *Mol. Phys.*, 1987, **60**, 193-203.
19. S. Kerisit and S. C. Parker, *J. Am. Chem. Soc.*, 2004, **126**, 10152-10161.
20. P. Raiteri, R. Demichelis and J. D. Gale, *J. Phys. Chem. C*, 2015, **119**, 24447-24458.